Research on 3D Radiation Fields Reconstruction based on FNN

Xu Wang [1, 2, a], Bin Li [2, b, *]

[1] School of Electronic and Information Engineering, Anhui University, Hefei, Anhui, 230601, China;

[2] School of Computer and Artificial Intelligence, Hefei Normal University, Hefei, Anhui, 230601, China.

[a] wangxu_2368@163.com, [b] libin11@mail.ustc.edu.cn

Abstract. Accurate radiation distribution could provide solid guidance for the protection of both occupational workers and the public. However, in some cases , such as nuclear accident, it is still hardly to obtain high accurate radiation distribution over the entire concerned region via numerical calculation due to complex geometry and/or radiation sources. In these cases, the radiation field reconstruction technique based on the limited measured and/or calculated radiation results has attracted more and more attention. In this work, an forward neural network (FNN) framework consisting of two fully connected layers connected by several residual blocks was proposed to study the reconstruction for 3D radiation with typical shielding layout including bulk shielding and streaming. With the help of the idea of piece-wise functions, a good prediction accuracy was achieved by dividing the entire zone into small training zone based on the magnitude of dose. The fraction of relative deviation between predicted and Monte Carlo results within 20% were 80.7% and 90% for bulking shielding case and the streaming case, respectively.

Keywords: radiation fields, shielding, dose, reconstruction, FNN.

1. Introduction

Radiation safety is widely considered as one of major bases of the development of nuclear energy and nuclear technology. The radiation distribution as detail as possible for the accessible area around nuclear facility can provide solid guidance for the protection to both occupational and public. The radiation distribution can be obtained by equipment measurements and numerical simulations. However, as the equipment is usually deployed at limited and sparse measurement positions in practice, it’s hardly to present the detail 3D radiation field via radiation monitoring. With the continuous development of particle transport solving algorithms (such as discrete ordinates method, Monte Carlo method) and computer technology, more and more advanced particle transport codes with parallel computing capabilities, such as MCNP[1], Serpent[2], OpenMC[3], NECP-MCX[4], JMCT[5], RMC[6],SCALE[7],PARTISN[8] and so on, have been developed. High-fidelity radiation distributions could be achieved by those tools in the condition of accurately modeling for geometry and radiation sources. However, in some cases, such as nuclear accident and hands-on operation during nuclear facility decommissioning and decontamination, it is still hardly to obtain high accurate radiation distribution with these codes due to the fact that it is difficult to accurately model the complex radiation source terms and/or geometry.In these cases, the radiation field reconstruction technique based on the limited measured and/or calculated radiation results has attracted more and more attention.

In general, these reconstruction techniques are based on interpolation algorithm or neural network model. Sai et al. (2016)[9] used multiquadric scattered data interpolation technique in gamma radiation field visualization. Wang et al proposed a method based on net function interpolation (2018)[10] and further developed it with Bayesian inference to reconstruct the neutron dose field (2020)[11]. Although above methods achieved good agreements between predictions and calculations, they only focused on the 2D radiation distribution. Zhu et al. (2022)[12] proposed a method using the modified Cahn-Hilliard equation to reconstruct 3D gamma dose field for radiation single source case. This method shows good agreement away from the source, but higher deviations near the source. Zhou et al. (2021)[13] developed an adaptive Back-propagation (BP) neural network method based on learning rate decay and applied it to reconstruct 2D photon flux and dose

distribution in a simple geometry model. Hao et al. (2023)[14] proposed an five-layer MLP network to reconstruct 3D photon radiation distribution in a simple geometry model.

In this work, the reconstruction of 3D radiation field for typical shielding layout (such as bulk shielding, streaming cases with forward neural network (FNN) will be studied. In the following sections, Section 2 will introduce the method of data preparation and neural network mode, and Section 3 will present the results and analysis for both single and multiple source cases.

2. Methodology

2.1 Date set preparation

In this work, the neutron dose distributions in a hypothetical plant with typical shielding layouts were calculated by the high-fidelity particle transport simulation based on Monte Carlo (MC) technique which can handle any complex geometry and employ the nuclear cross-section data without any severe approximations, to be used for neural network training and validation. In dose distribution simulation, an open source MC-based particle transport code OpenMC developed at MIT was used together with ENDF/B-VII.1[15] nuclear cross section library and the fluence-to-dose conversion factors from ICRP 74[16]

The hypothetical plant consists of two rooms, as shown in Fig. 1. A shielding chamber with the concrete walls (0.2m thickness in west and east, 0.1m thickness in south and north), located at the northeast corner of the Room A, is used for studying the bulk shielding effect. On the south wall of the shielding chamber, a square hole with dimensions of 10cm by 10cm (1 meter above the ground) is opened to simulate the leakage beam effect caused by hole penetrating parts and other similar effects.

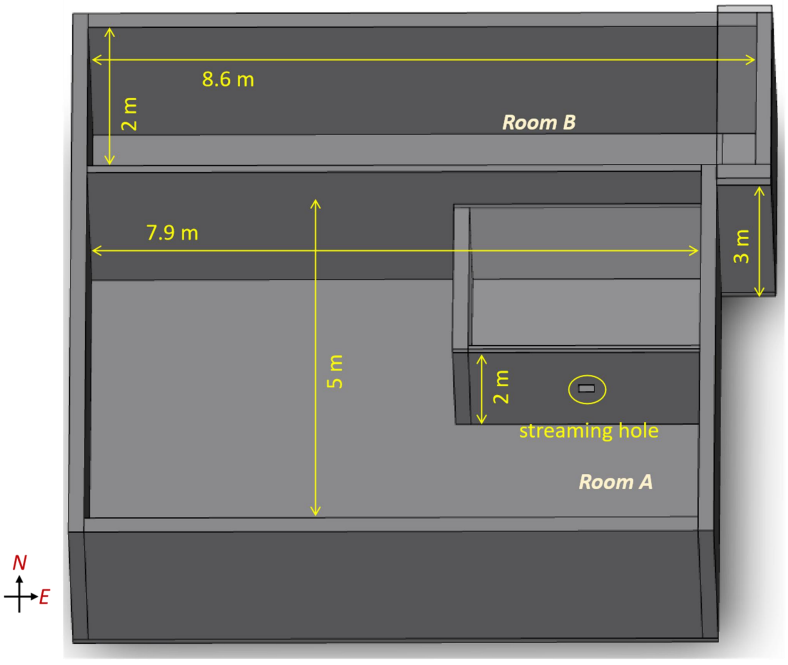

Fig. 1 Layout of hypothetical plant

2.2 Neural network model

In machine learning, the radiation field reconstruction technique can be classified as a regression problem. Therefore, a framework based on FNN was built in present work. The framework is composed of two fully-connected (FC) layers connected by several residual blocks, as shown in Fig.2. To avoid gradient vanishing during backward propagation, the shortcut in residual block will be activated only when the hidden layers (e.g. the number of res blocks) is greater and/or equal 10.

To improve the flexibility of framework, the model layers and number of nodes in each layer can be specified by the user.

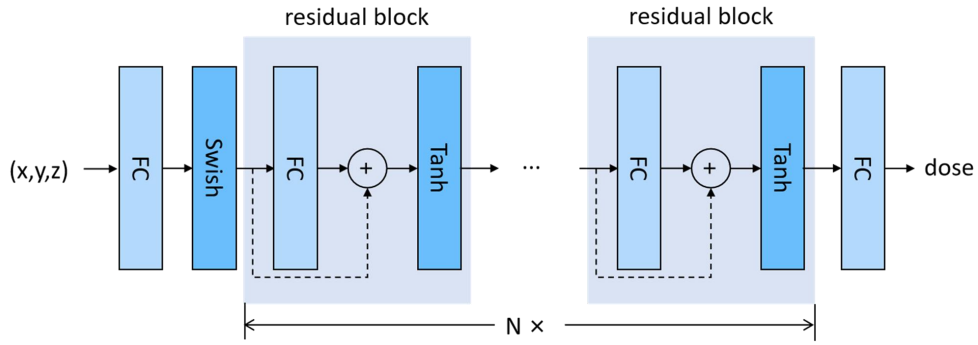

Fig. 2 Framework of network for reconstructing 3D radiation field

The hyperbolic tangent function (e.g. tanh(x), as shown in Fig. 3), which transforms the inputs to outputs lie on the interval (-1,1) and approaches a linear transformation around zero input, is used as activation function in the res block. As shown in Fig. 3, as tanh(x) varies slowly within range of $|x| > 2$ (in other words, the derivative of the tanh function approaches 0 in this interval), both the inputs (e.g. spatial coordinates) and labels (e.g. doses) are pre-pocessed with Z-score normalization, which transforms the data set $\{x^{(n)}\}_{n=1}^{N}$ to the data set with mean of zero and variance of one, as following

$$\hat{x}^{(n)} = \frac{x^{(n)} - \mu}{\sigma} \tag{1}$$

where

$$\mu = \frac{1}{N}\sum_{n=1}^{N} x^{(n)} \tag{2}$$

$$\sigma^2 = \frac{1}{N-1}\sum_{n=1}^{N} \left(x^{(n)} - \mu\right)^2 \tag{3}$$

The weights of model are initialized with Xavier method instead of default method (Kaiming Uniform)

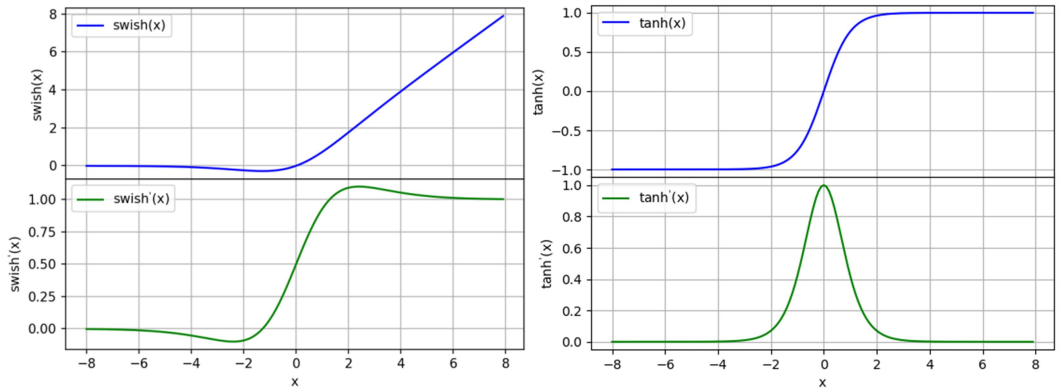

Fig. 3 Swish(x) and Tanh(x) and their first derivative

And the Adam optimization with learning rate of 1.0e-4 was adopted, and to suppress the over-fit effect as soon as possible, L2 regularization was used

3. Results and Analysis

In present work, a isotropic cuboid source with size of 21.42 cm and height of 1.5 m was deployed at the center of shielding chamber.

3.1 Case 1: bulk shielding

To study only bulk shielding, the streaming in the model described in Section 2.1 were neglected. The radiation field data calculated by MC code with this modified model was used to train and validate neural network.

Previous studies show the selection of train data has great effectiveness on the prediction ability of network. Thus, to improve the generation ability of network, the principle for selecting train set samples is to make the data distribution feature on train set and validation set as close as possible. In this work, with the bottom center of radiation source as origin of R-Z-Theta coordinate system, several points randomly were sampled in theta of and z along the different radius as train set, as shown in Fig. 4. The remain data belong validation set

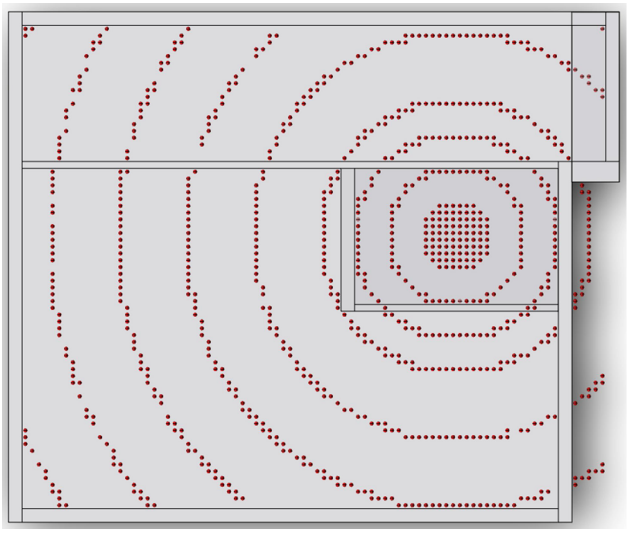

Fig. 3 Spatial distribution of coordinate of samples in train set

Based on the above train set and validation set, we initially tried to build a deep neural network which has good predicted ability on the whole plant space. However, it was found the fraction of relative deviation within 20% between the predicted and MC results hardly exceeds 50% and the predicted data only around the source shown good agreement with the MC results, although the layers of network is 9 and total nodes is as high as 10272.

Considering that a deeper neural network may result in the potential over-fitting effect, with the help of the idea of piece-wise functions, we divided the entire space into a number of small regions and use a smaller-scale neural network to reconstruct each small region. With this method, for bulk shielding case, a 7 layers network with the nodes of 200 and a 7 layers network with the nodes of 4500 were built to reconstruct the field in the shielding chamber and the remain space, separately. About 82.7% of fraction of relative deviation within 20% over the entire space was achieved, as shown in Table 1. The comparison of radiation field distribution was presented in Fig.4, showing a good agreement between predicted and MC results. Besides, it can be also found that the larger deviations occur where the dose is smaller, indicating that predicted accuracy could be further improved by dividing more sub-train zones.

Table 1. Summary of network for reconstructing radiation fields in bulk shielding case

Target Zone	Structure of network	Train set		Validation set		Entire space	
		Samples	Fraction of Δ≤20%	Samples	Fraction of Δ≤20%	Samples	Fraction of Δ≤20%
Shielding chamber	50,40,30,30,20,20,10	493	0.94	10508	0.91		
Remain space	100, 200, 500, 1000, 2000, 500, 200	2993	0.88	160195	0.82		
						175188	0.827

Δ=abs(P-C)/C, where C stands for MC calculated , P stands for predicted.

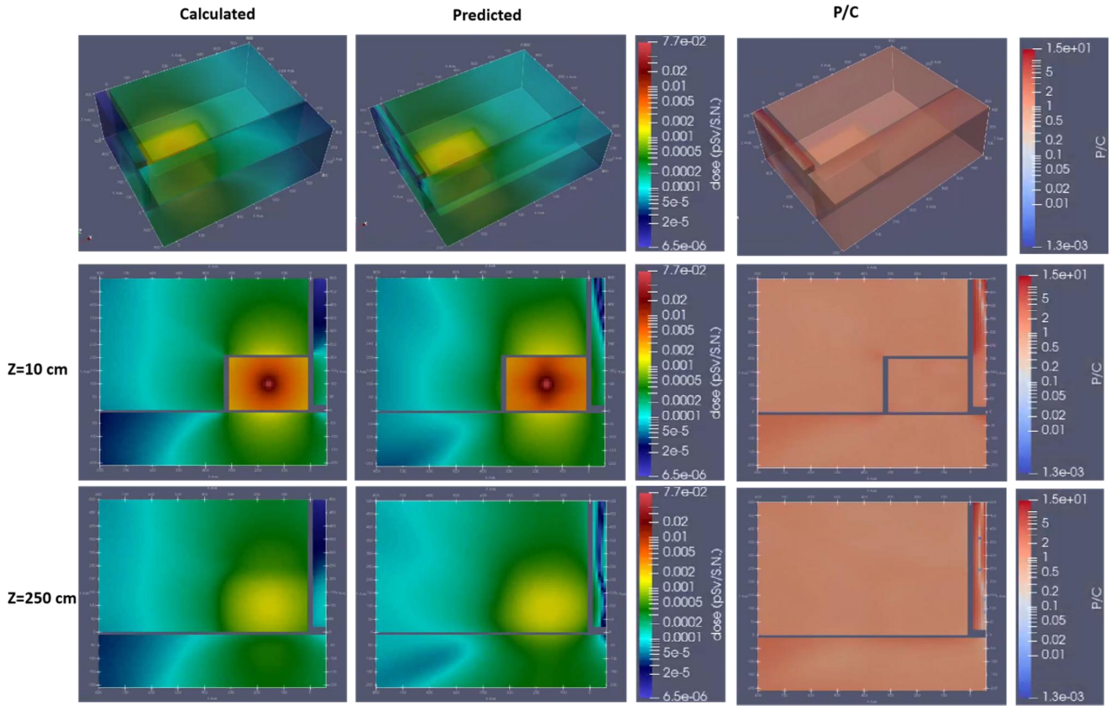

Fig. 4 Comparison of MC results and predicted for bulk shielding

3.2 Case 2: streaming

In this case, to study the reconstruction for radiation field with streaming, a square hole was opened at the southern wall of the shielding chamber, as shown in Fig.1. With the same network structure and spatial partition policy as the Case 1, the accuracy in this case is not as good as the result of Case 1. The results are listed in Table 2 and the distribution comparison are present in the Fig.5.

Table 2. Summary of network for reconstructing radiation fields in streaming case

Target Zone	Structure of network	Train set		Validation set		Entire space	
		Samples	Fraction of Δ≤20%	Samples	Fraction of Δ≤20%	Samples	Fraction of Δ≤20%
Shielding chamber	50,40,30,30, 20,20,10	493	0.95	10508	0.90		
Remain space	100, 200, 500, 1000, 2000, 500, 200	2993	0.85	158455	0.75		
						168963	0.759

Δ=abs(P-C)/C, where C stands for MC calculated , P stands for predicted.

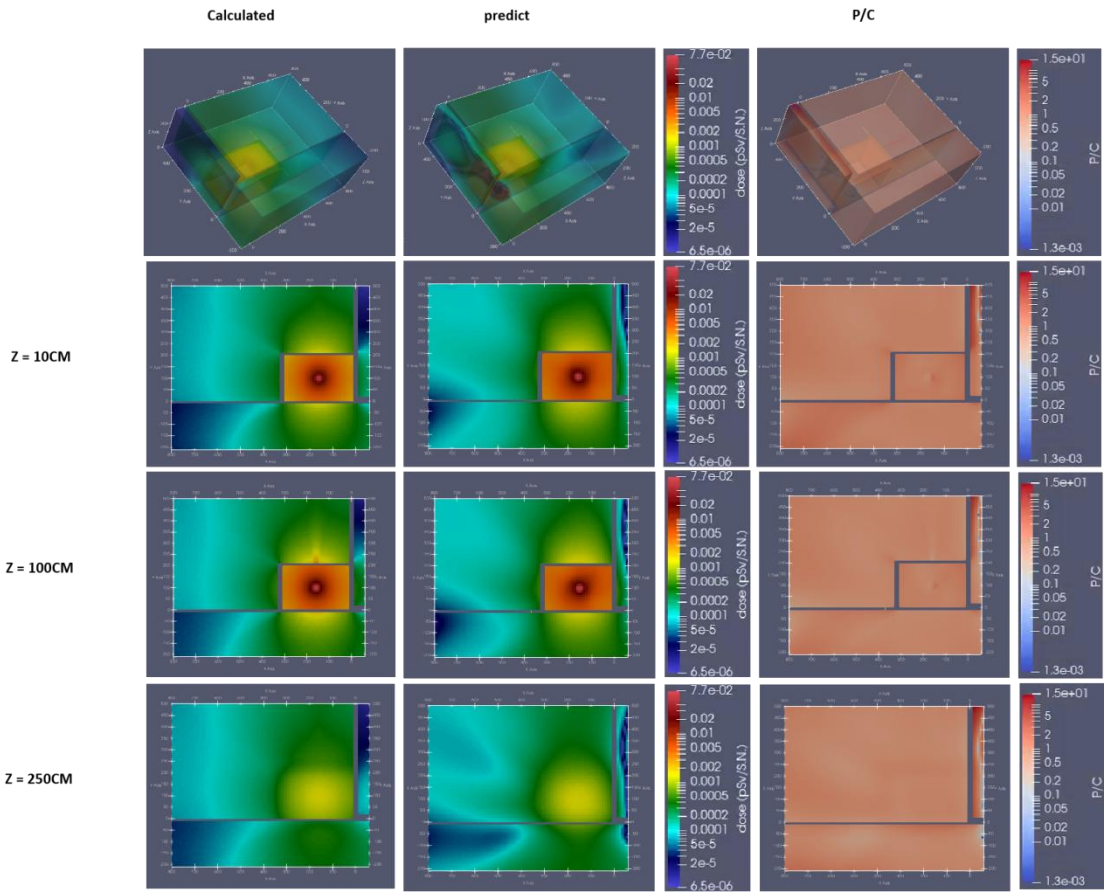

Fig. 5 Comparison of MC results and predicted for bulk shielding and streaming(2 training areas)

We think that the model complexity increases after the streaming region is added, and training outside the radiation source room as a whole will make the fitted function more complex, resulting in lower training effect than case1. Therefore, we further divide the region outside the radiation source room into two smaller regions: Radiate the area due south of the room and the rest of the area,as shown in the Fig 6. Using this method, the regions with large changes in radiation characteristics are divided, and the predicted results are shown in Table 3

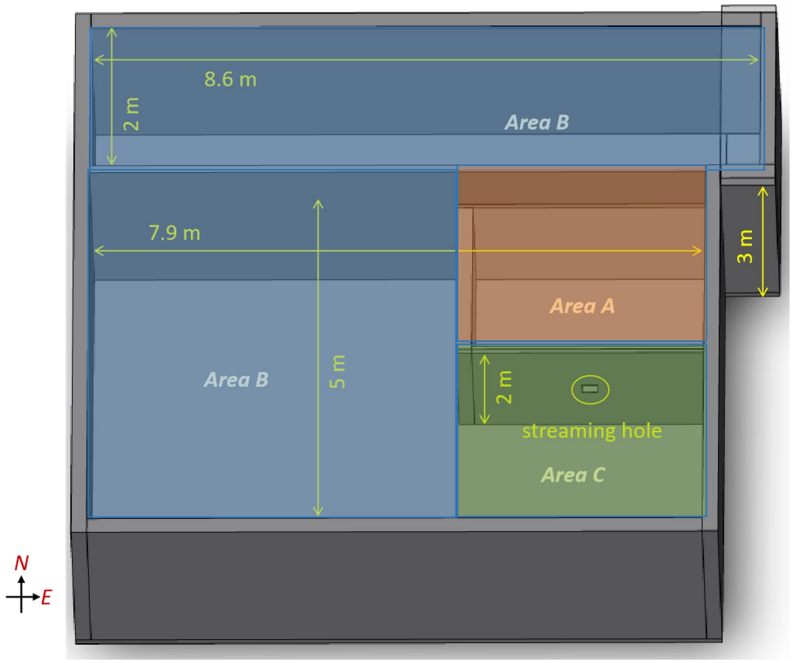

Fig. 6 Case where streaming is divided into three regions

Table 3. Summary of radiation field divided into three regions in streaming case

Target Zone	Structure of network	Train set		Validation set		Entire space	
		Samples	Fraction of Δ≤20%	Samples	Fraction of Δ≤20%	Samples	Fraction of Δ≤20%
Area A	50,40,30,30,20 ,20,10	493	0.96	10508	0.916		
Area B	100, 200, 500, 1000, 2000, 500, 200	2993	0.85	131615	0.807		
Area C	50,40,30,30,20 ,20,10	493	1	27348	0.994		
						169305	0.844

Δ=abs(P-C)/C, where C stands for MC calculated , P stands for predicted.

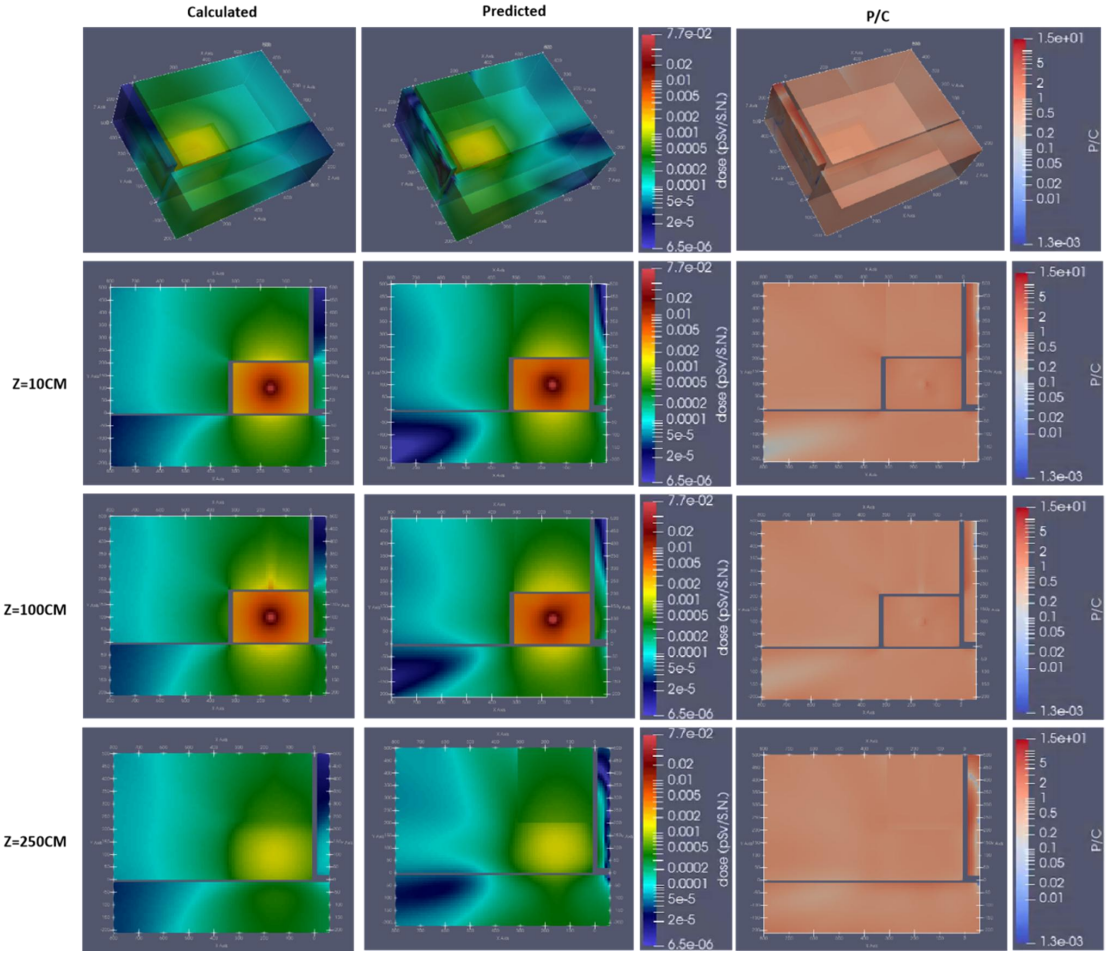

Fig. 7 Comparison of MC results and predicted for bulk shielding and streaming(3 training areas)

In addition, it can be seen from Fig 5 and Fig 7 that a large part of the area causing prediction errors stems from the northwest direction of the model, because it is far away from the radiation source and receives the effect of absorption and reflection from the wall, so the radiation dose value changes more complicated. If the prediction ability of this region can be improved, then the overall prediction ability of FNN can be further improved.

With idea of sub-regional training, Room B was further divided into two sub-regions, as shown in Fig 8. The radiation results predicted by this segmentation method are shown in Table 4 and Fig 9.

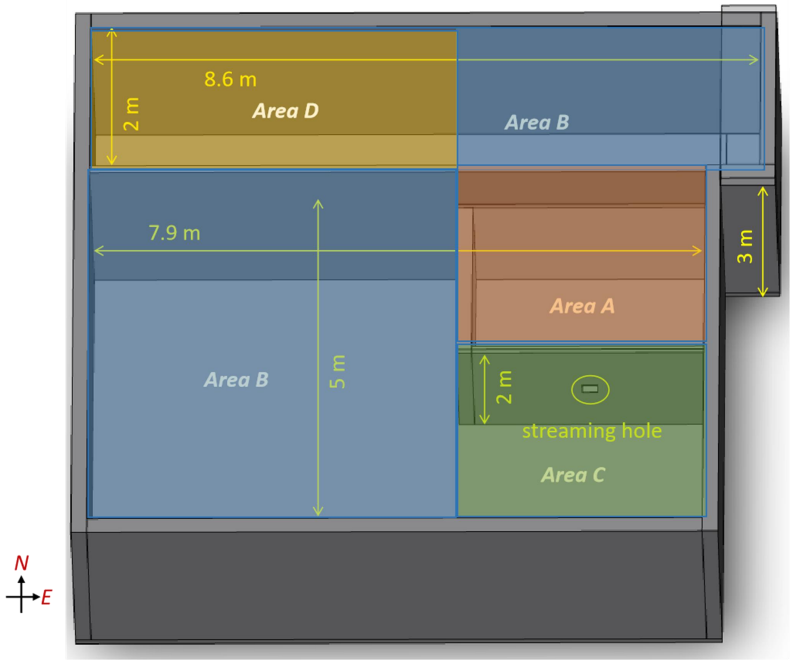

Fig. 8 Case where streaming is divided into four regions

Table 4. Summary of radiation field divided into four regions in streaming case

Target Zone	Structure of network	Train set		Validation set		Entire space	
		Samples	Fraction of Δ≤20%	Samples	Fraction of Δ≤20%	Samples	Fraction of Δ≤20%
Area A	50,40,30,30, 20,20,10	493	0.96	10508	0.916		
Area B	100, 200, 500, 1000, 2000, 500, 200	2993	0.9	105655	0.85		
Area C	50,40,30,30, 20,20,10	493	1	27348	0.994		
Area D	50,40,30,30, 20,20,10	493	1	27708	0.994		
						171219	0.9

Δ=abs(P-C)/C, where C stands for MC calculated , P stands for predicted.

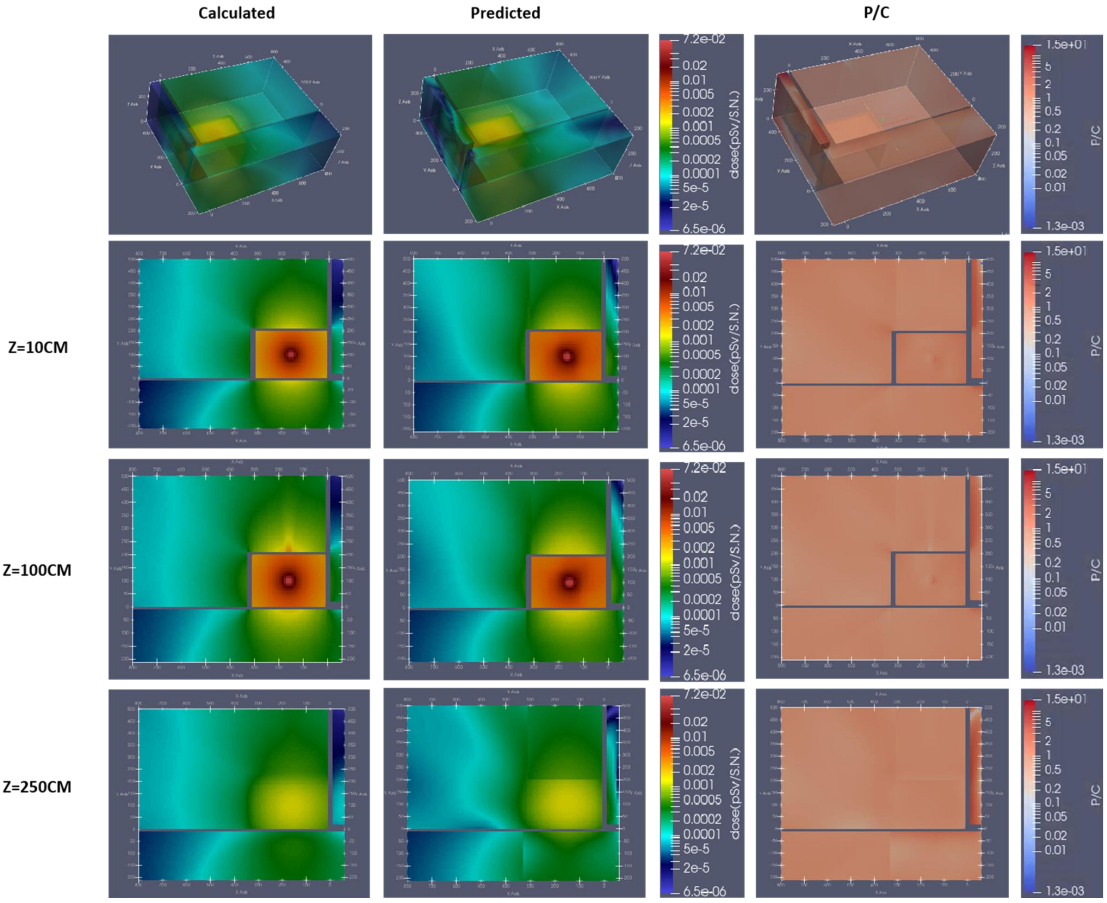

Fig. 9 Comparison of MC results and predicted for bulk shielding and streaming(4 training areas)

4. Summary

This work investigates a neural network-based methodology for reconstructing 3D radiation fields in nuclear facilities with limited measurements. The study utilizes Monte Carlo simulations to generate neutron dose distributions for training and validating the forward neural network (FNN). The FNN incorporates residual blocks and advanced optimization techniques to mitigate gradient vanishing and overfitting. During training, it was found that the deeper neural networks didn't work well in predictions accuracy. Based on the idea of piece-wise function, dividing the entire space into a number of small regions and using a smaller-scale neural network to reconstruct each small region can achieve good results in the whole space. The reconstructions for radiation fields of two typical shielding layout including bulk shielding and streaming were performed. In bulk shielding case, by dividing the radiation field into two sub-regions, the fraction of relative deviations within 20% for entire space was achieved 82%. In the streaming case, further subdivision of regions reduces prediction complexity and improves accuracy in areas with significant radiation variations,the overall accuracy was more than 84% when the deviation was less than 20 percent. For the area with large deviation, it is further divided into independent zones, reaching 90% accuracy over entire space. The results highlight the efficiency of the FNN framework in handling complex radiation fields and provide a foundation for its application in nuclear safety assessments and accident responses.

In the future, the reconstructions for 3D radiation fields with more shielding layout such as maze, shadow shielding will be studied. And the network structure could be further optimized.

Acknowledgement

This work was supported by the Hefei Normal University 2022 High-level Talent Scientific Research Start-up Fund Project (No. 2022rcjj51) and National Natural Science Foundation of China (No. 11905247).

References

[1] Kulesza J , Adams T , Armstrong J, et al.MCNP Code Version 6.3.0 Theory & User Manual[R]. 2022.DOI:10.2172/1889957.

[2] Valtavirta,Ville,Kaltiaisenaho,et al.The Serpent Monte Carlo code: Status, development and applications in 2013[J].Annals of nuclear energy, 2015.DOI:10.1016/j.anucene.2014.08.024.

[3] A P K R , A N E H , A B R H ,et al.OpenMC: A state-of-the-art Monte Carlo code for research and development[J].Annals of Nuclear Energy, 2015, 82:90-97.DOI:10.1016/j.anucene.2014.07.048.

[4] He Q , Zheng Q , Li J ,et al.NECP-MCX: A hybrid Monte-Carlo-Deterministic particle-transport code for the simulation of deep-penetration problems[J].Annals of Nuclear Energy, 2021, 151:107978.DOI:10.1016/j.anucene.2020.107978.

[5] Deng, L., Li, G., Zhang, BY. et al. A high fidelity general purpose 3-D Monte Carlo particle transport program JMCT3.0[J]. Nuclear Science and Techiques 33, 108 (2022). https://doi.org/10.1007/s41365-022-01092-0.

[6] Wang K , Li Z , She D ,et al.RMC - A Monte Carlo code for reactor core analysis[J].Annals of nuclear energy, 2015(82-Aug.).DOI:10.1016/j.anucene.2014.08.048.

[7] W.A. Wieselquist, R. A. Lefebvre, Eds. SCALE6.3.2 User Manual[R], ORNL/TM-2024/3386, UT-Battelle, Oak Ridge National Laboratory(February 2024).

[8] Baker R S .Time-Dependent, Parallel Neutral Particle Transport Code System[R]. LA-UR-08-07258, 2009.

[9] Sai X , Chen Y , Wei M .Preliminary application of Multiquadric scattered data interpolation technique in gamma radiation field visualization[J].Nuclear Techniques, 2016.DOI:10.11889/j.0253-3219.2016.hjs.39.100501.

[10] Wang Z , Cai J .Inversion of radiation field on nuclear facilities: A method based on net function interpolation[J].Radiation Physics and Chemistry, 2018, 153:27-34.DOI:10.1016/j.radphyschem.2018.09.003.

[11] Wang Z , Cai J .Reconstruction of the neutron radiation field on nuclear facilities near the shield using Bayesian inference[J].Progress in Nuclear Energy, 2020, 118:103070-.DOI:10.1016/j.pnucene.2019.103070.

[12] Zhu S , Zhuang S ,Fang, ShengDong, XinwenLi, WenqianZhang, LeiLiu, XinkaiLi, RenLiu, XuegangCao, Jianzhu.3-D gamma radiation field reconstruction method using limited measurements for multiple radioactive sources[J].Annals of nuclear energy, 2022, 175(Sep.):109245.1-109245.14.DOI:10.1016/j.anucene.2022.109247.

[13] Zhou W, Sun G, Yang Z, et al. BP neural network based reconstruction method for radiation field applications[J]. Nuclear Engineering and Design, 2021, 380: 111228.

[14] Yisheng H, Zhen W, Yanheng P, et al. Validation of the neural network for 3D photon radiation field reconstruction under various source distributions[J]. Frontiers in Energy Research, 2023, 11: 1151364

[15] Chadwick.M.B,Herman.M,et al.ENDF/B-VII.1 Nuclear Data for Science and Technology: Cross Sections, Covariances, Fission Product Yields and Decay Data[J].Nuclear Data Sheets,2011,112(Dec):2887-2996.DOI:10.1016/j.nds.2011.11.002.

[16] International Commission on Radiological Protection, Protection against Neutron Radiation[R], ICRP Publication 74, 1996.